Impact parameter dependence of collective flow and its disappearance for different mass asymmetries.

Supriya Goyal

Department of Physics, Panjab University, Chandigarh 160 014, India

E-mail: `ashuphysics@gmail.com`

Abstract. We study the role of impact parameter on the collective flow and its disappearance for different mass asymmetric reactions. The mass asymmetry is varied from 0 to 0.7 keeping the total mass of the system fixed. Our results clearly indicate a significant role of impact parameter on the collective flow and its disappearance for the mass asymmetric reactions. The impact parameter dependence is also found to vary with mass asymmetry of the reaction.

1. Introduction

On the collision of two nuclei, the density and pressure increases in the interaction region and at finite colliding geometries, there is an inherent asymmetry in the pressure which results in a collective transverse flow of matter toward the direction of lowest pressure. This collective transverse flow is one of the most extensively used observable to study the equation of state (EoS) as well as in-medium nucleon-nucleon (nn) cross-section of the nuclear matter. At the particular value of energy where the attractive scattering (dominant at energies around 10 MeV/nucleon) balances the repulsive interactions (dominant at energies around 400 MeV/nucleon), collective transverse flow in the reaction plane disappears. This energy is termed as Balance Energy (E_{bal}) [1, 2, 3, 4, 5, 6, 7, 8, 9, 10].

Both collective flow and E_{bal} are found to be highly sensitive towards the nn cross-section [2, 3, 4, 5, 6, 7, 8, 9, 10], size of the system ($A_{TOT} = A_T + A_P$; where A_T and A_P are the masses of the target and projectile, respectively) [4], mass asymmetry of the reaction ($\eta = \frac{A_T - A_P}{A_T + A_P}$) [11], nuclear matter equation of state [2, 3, 4, 5, 6, 7, 8, 9, 10], incident energy (E MeV/nucleon) [12] as well as the colliding geometry ($\hat{b} = \frac{b}{b_{max}}$; where $b_{max} = R_1 + R_2$; R_i is the radius of projectile or target) [2, 5, 7, 9, 10]. Several experimental and theoretical attempts have been employed in order to explain and understand these observations [1, 2, 3, 4, 5, 6, 7, 8, 9, 10, 11, 12]. Due to the decrease in the compression reached in heavy-ion collisions with increase in the impact parameter, E_{bal} is found to increase approximately linearly as a function of the impact parameter [13, 14]. But most of the studies in the literature mainly focus on the symmetric and nearly symmetric reactions. Our present aim, therefore, is at least twofold. (1) To study the variation of collective transverse flow with impact parameter for different η keeping the incident energy fixed. (2) To study the sensitivity of collective transverse flow and its disappearance on the mass asymmetry of the reaction at different impact parameters. The Quantum Molecular Dynamics (QMD) model [8, 15, 16] used for the present analysis is explained in the section 2. Results and discussion are presented in section 3 followed by summary in section 4.

2. Description of the model

In the QMD model, each nucleon propagates under the influence of mutual two- and three-body interactions. The propagation is governed by the classical equations of motion:

$$\frac{d\vec{r_i}}{dt} = \frac{dH}{d\vec{p_i}}, \tag{1}$$

$$\frac{d\vec{p_i}}{dt} = -\frac{dH}{d\vec{r_i}}, \tag{2}$$

where the Hamiltonian is given by

$$H = \sum_i \frac{\vec{p_i^2}}{2m_i} + V^{tot}. \tag{3}$$

Our total interaction potential V^{tot} reads as [8, 15, 16]

$$V^{tot} = V^{Loc} + V^{Yuk} + V^{Coul}, \tag{4}$$

with

$$V^{Loc} = t_1\delta(\vec{r_i} - \vec{r_j}) + t_2\delta(\vec{r_i} - \vec{r_j})\delta(\vec{r_i} - \vec{r_k}), \tag{5}$$

$$V^{Yuk} = t_3 e^{-|\vec{r_i}-\vec{r_j}|/m} / \left(|\vec{r_i} - \vec{r_j}|/m\right), \tag{6}$$

with m = 1.5 fm and t_3 = -6.66 MeV.

The static (local) Skyrme interaction can further be parametrized as:

$$U^{Loc} = \alpha \left(\frac{\rho}{\rho_o}\right) + \beta \left(\frac{\rho}{\rho_o}\right)^\gamma. \tag{7}$$

Here α, β and γ are the parameters that define equation of state. The parameters α, β, and γ in above Eq. (7) must be adjusted so as to reproduce the ground state properties of the nuclear matter. The set of parameters corresponding to different equations of state can be found in Ref. [16]. It is worth mentioning that as shown by Puri and coworkers, Skyrme forces are very successful in the analysis of low energy phenomena such as fusion, fission and cluster-radioactivity, where nuclear potential plays an important role [17].

3. Results and Discussion

For the present study, we simulated the reactions of $^{20}_{10}Ne +^{20}_{10}Ne$ ($\eta = 0$), $^{17}_{8}O +^{23}_{11}Na$ ($\eta = 0.1$), $^{14}_{7}N +^{26}_{12}Mg$ ($\eta = 0.3$), $^{10}_{5}B +^{30}_{14}Si$ ($\eta = 0.5$), and $^{6}_{3}Li +^{34}_{16}S$ ($\eta = 0.7$) for total mass (A_{TOT}) = 40, $^{40}_{20}Ca +^{40}_{20}Ca$ ($\eta = 0$), $^{36}_{18}Ar +^{44}_{20}Ca$ ($\eta = 0.1$), $^{28}_{14}Si +^{52}_{24}Cr$ ($\eta = 0.3$), $^{20}_{10}Ne +^{60}_{28}Ni$ ($\eta = 0.5$), and $^{10}_{5}B +^{70}_{32}Ge$ ($\eta = 0.7$) for total mass (A_{TOT}) = 80, $^{80}_{36}Kr +^{80}_{36}Kr$ ($\eta = 0$), $^{70}_{32}Ge +^{90}_{40}Zr$ ($\eta = 0.1$), $^{54}_{26}Fe +^{106}_{48}Cd$ ($\eta = 0.3$), $^{40}_{20}Ca +^{120}_{52}Te$ ($\eta = 0.5$), and $^{24}_{12}Mg +^{136}_{58}Ce$ ($\eta = 0.7$) for total mass (A_{TOT}) = 160, and $^{120}_{52}Te +^{120}_{52}Te$ ($\eta = 0$), $^{108}_{48}Cd +^{132}_{56}Ba$ ($\eta = 0.1$), $^{84}_{38}Sr +^{156}_{66}Dy$ ($\eta = 0.3$), $^{60}_{28}Ni +^{180}_{74}W$ ($\eta = 0.5$), and $^{36}_{18}Ar +^{204}_{82}Pb$ ($\eta = 0.7$) for total mass (A_{TOT}) = 240. The impact parameter is varied from b/b$_{max}$ = 0 to 1 in small steps of 0.25. The charges are chosen in a way so that colliding nuclei are stable nuclides. A soft equation of state with isotropic energy dependent cugnon cross-section (labeled as Soft^{iso}) is used for the present calculations.

The balance energy (E_{bal}) is calculated using the *directed transverse momentum* $< P_x^{dir} >$, which is defined as:

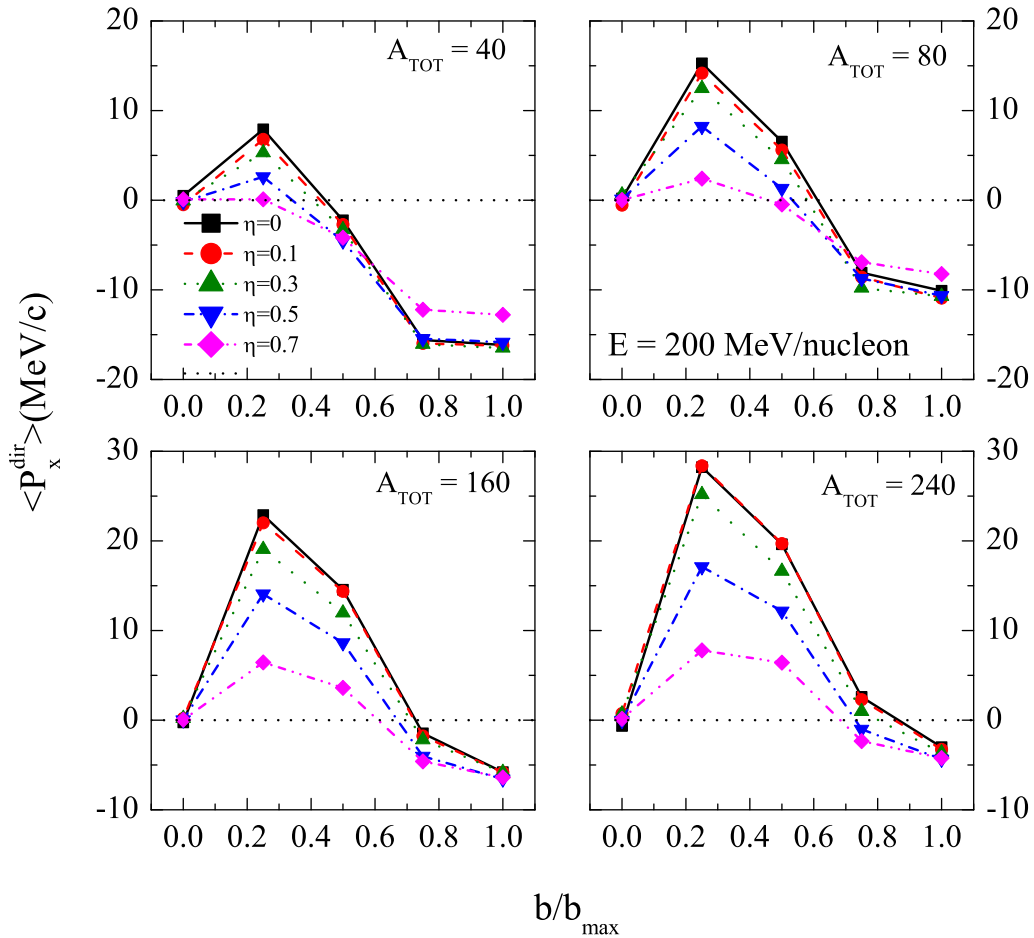$$\langle P_x^{dir} \rangle = \frac{1}{A} \sum_i \text{sign}\{Y(i)\} \, \mathbf{p}_x(i), \tag{8}$$

Figure 1. (Color online) The $< P_x^{dir} >$ (MeV/c) as a function of reduced impact parameter (b/b_{max}) for different system masses. The results for different mass asymmetries $\eta = 0, 0.1, 0.3, 0.5,$ and 0.7 are represented, respectively, by the solid squares, circles, triangles, inverted triangles, and diamonds. Results are at an incident energy of 200 MeV/nucleon.

where $Y(i)$ and $\mathbf{p}_x(i)$ are the rapidity distribution and transverse momentum of ith particle, respectively.

In Fig. 1, we display at a fixed energy, the $< P_x^{dir} >$ as a function of reduced impact parameter (b/b_{max}) for $\eta = 0$-0.7, keeping total system mass fixed as 40, 80, 160, and 240. All reactions are followed till 200 fm/c, where $< P_x^{dir} >$ saturates. In all cases $< P_x^{dir} >$ first increases with increase in impact parameter, reaches a maximal value and after passing through a zero at some intermediate value of impact parameter, attains negative values. The trend is uniform throughout the mass asymmetry range. The value of impact parameter at which $< P_x^{dir} >$ attains a zero (which is termed as Geometry of Vanishing Flow (GVF) [18]) varies with η and A_{TOT}. For lighter systems and larger η, the value of GVF is smaller compared to the heavier systems and smaller η.

In Fig. 2, the variation of GVF as a function of η is displayed for different system masses. The percentage variation in GVF while going from $\eta = 0$ to 0.7 is -40.9%, -24.59%, -16.44%, and -20.93%, respectively for $A_{TOT} = 40, 80, 160,$ and 240. It is clear from the figure that the effect of mass asymmetry of the reaction on GVF decreases with increase in system mass. This
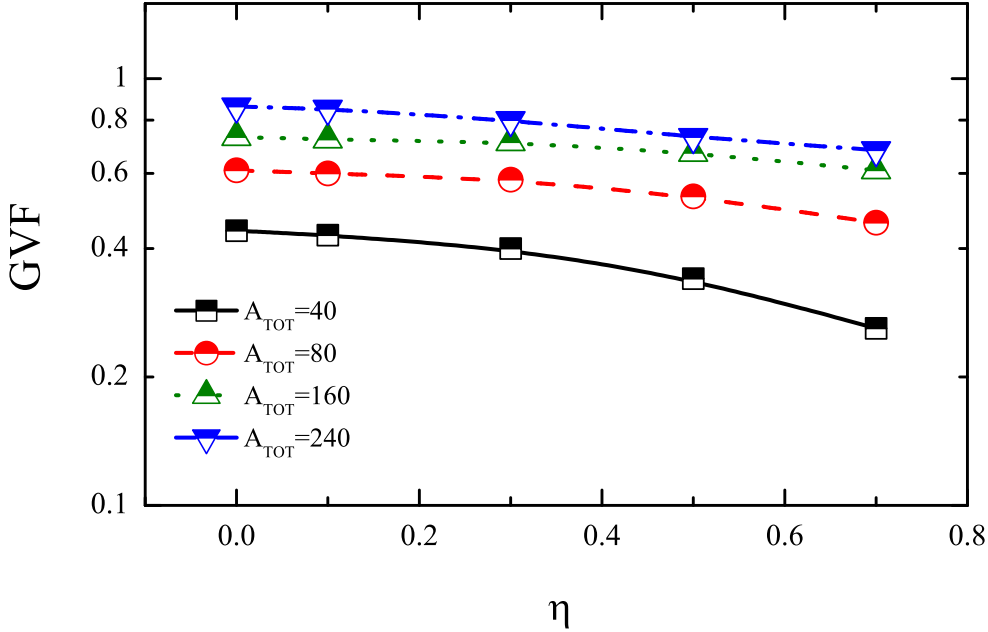
Figure 2. (Color online) The geometry of vanishing flow (GVF) as a function of η for different system masses. The results for different system masses (A_{TOT}) = 40, 80, 160, and 240 are represented, respectively, by the half filled squares, circles, triangles, and inverted triangles.

is similar to as predicted for E_{bal} [11]. Due to the decrease in nn collisions with increase in η and impact parameter and increase in Coulomb repulsion with increase in A_{TOT}, the E_{bal} increases with increase in η and impact parameter, while it decreases with increase in A_{TOT}. Since the present study is at fixed incident energy, therefore, the value of impact parameter, where flow vanishes, decreases as η increases.

In Fig. 3, we display $< P_x^{dir} >$ as a function of incident energy ranging between 40 MeV/nucleon and 800 MeV/nucleon, for different mass asymmetric reactions keeping the total mass of the system fixed as 240. The results are shown for different impact parameters. In all the cases, transverse momentum is negative at lower incident energies which turns positive at relatively higher incident energies. The value of the abscissa at zero value of $< P_x^{dir} >$ corresponds to the balance energy. The figure indicates that (i) for all values of η and impact parameters, the transverse momentum increases monotonically with increase in the incident energy. The increase is sharp at smaller incident energies compared to higher incident energies where it starts saturating. (ii) due to decrease in overlap volume and hence number of collisions with increase in η, the transverse momentum starts suppressing as η increases and hence the balance energy increases with increase in η. (iii) the variation in $< P_x^{dir} >$ with η decreases with increase in impact parameter. But with increase in impact parameter the balance energy increases for all values of η.

The above mentioned findings can be understood by decomposing the total transverse momentum into contributions due to mean field and two- body nn collisions as shown in Fig. 4. The symbols are explained in the caption of the figure. One notices that mean field flow increases up to couple of hundred MeV/nucleon and then saturates. In the lower incident energy region, the flow due to mean field is smaller for larger asymmetries compared to smaller asymmetries. At higher incident energies the mean field flow is nearly independent of η. Similar behavior is seen
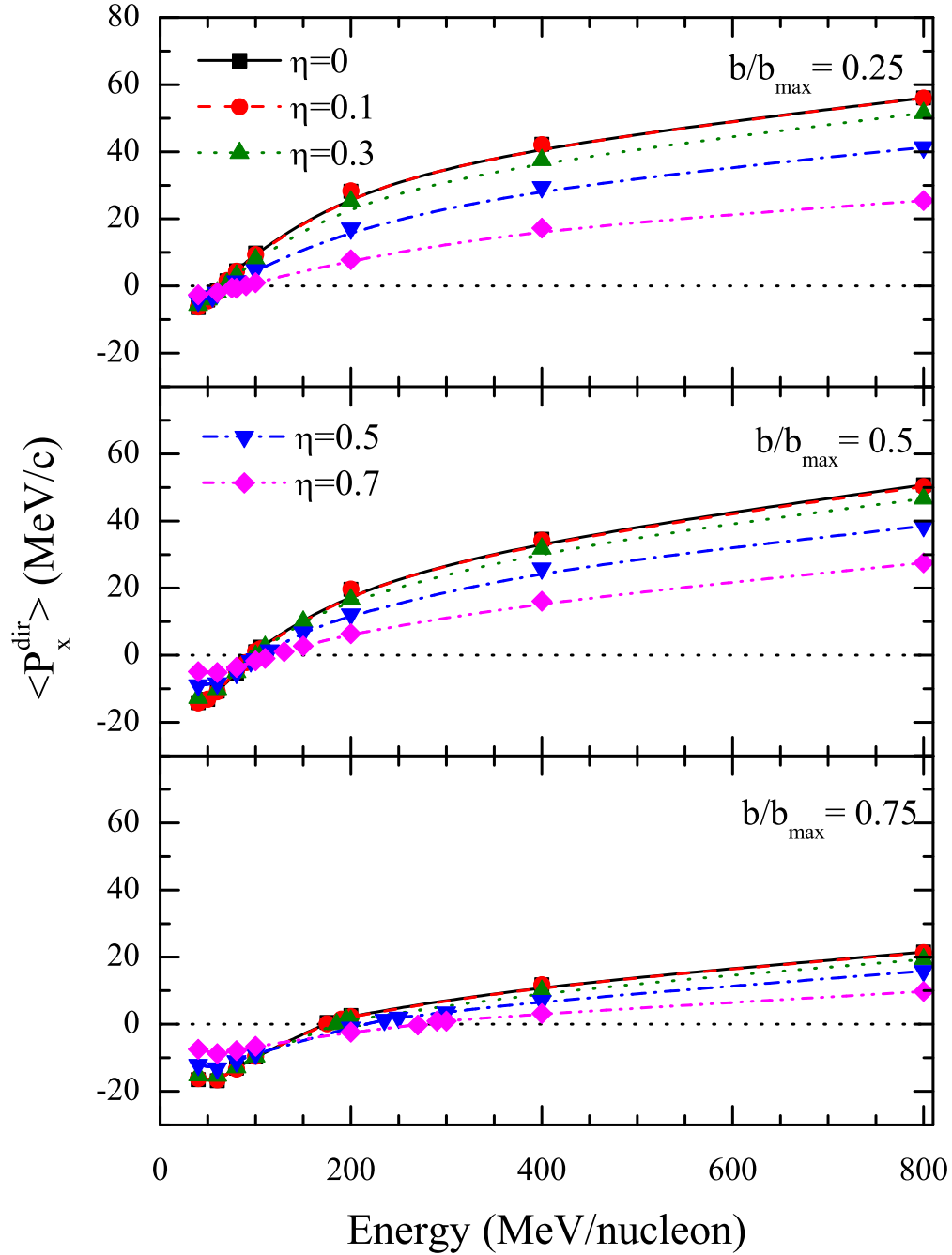
Figure 3. (Color online) The $< P_x^{dir} >$ (MeV/c) as a function of incident energy for system mass $A_{TOT} = 240$. The results are shown for different mass asymmetries ($\eta = 0$-0.7) at reduced impact parameters $b/b_{max} = 0.25$ (upper panel), 0.5 (middle panel), and 0.75 (bottom panel). The lines are only to guide the eye. Symbols have the same meaning as in Fig. 1.
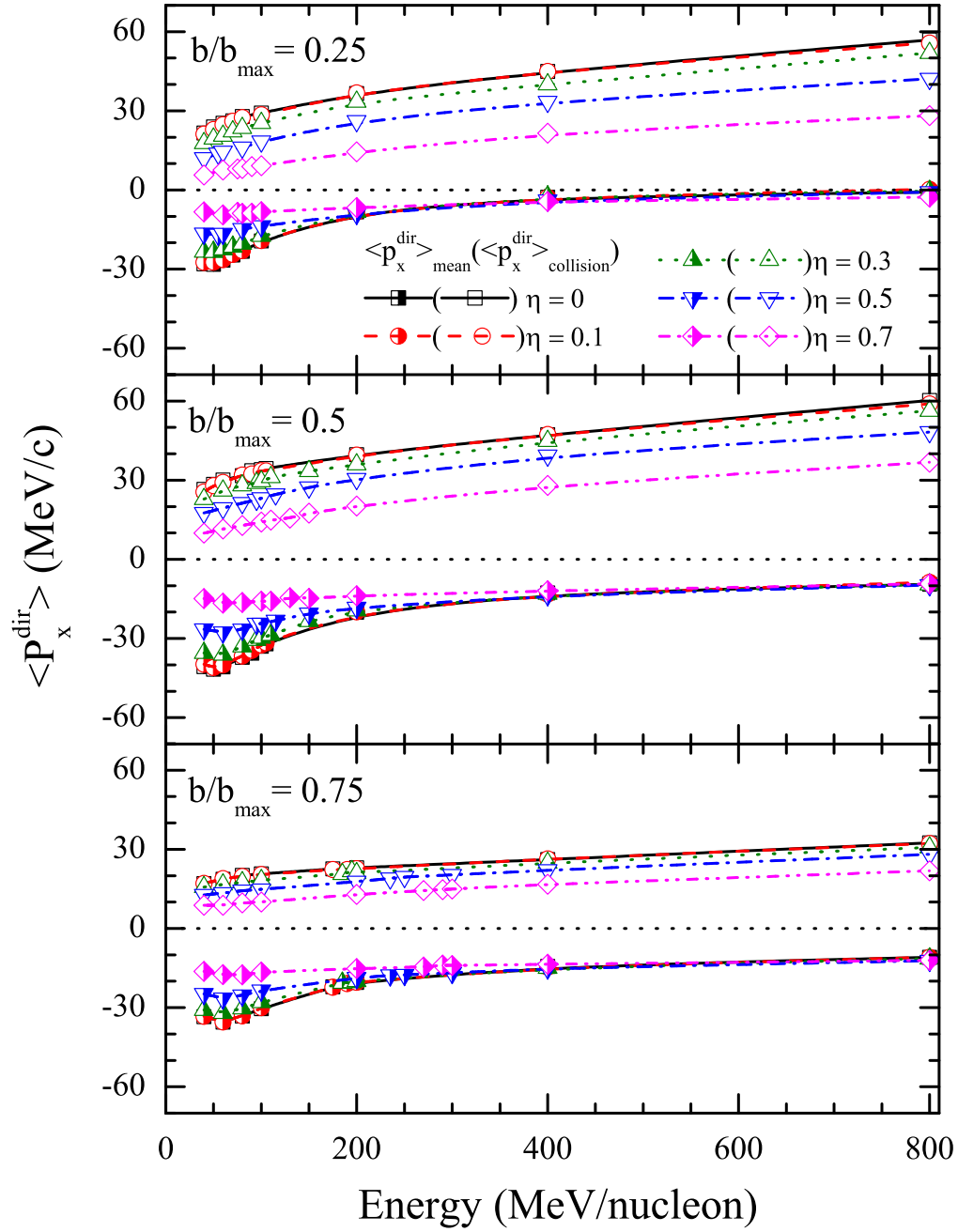
Figure 4. (Color online) The decomposition of $< P_x^{dir} >$ displayed in Fig. 3 into mean field (half filled symbols) and collision part (open symbols) as a function of incident energy.

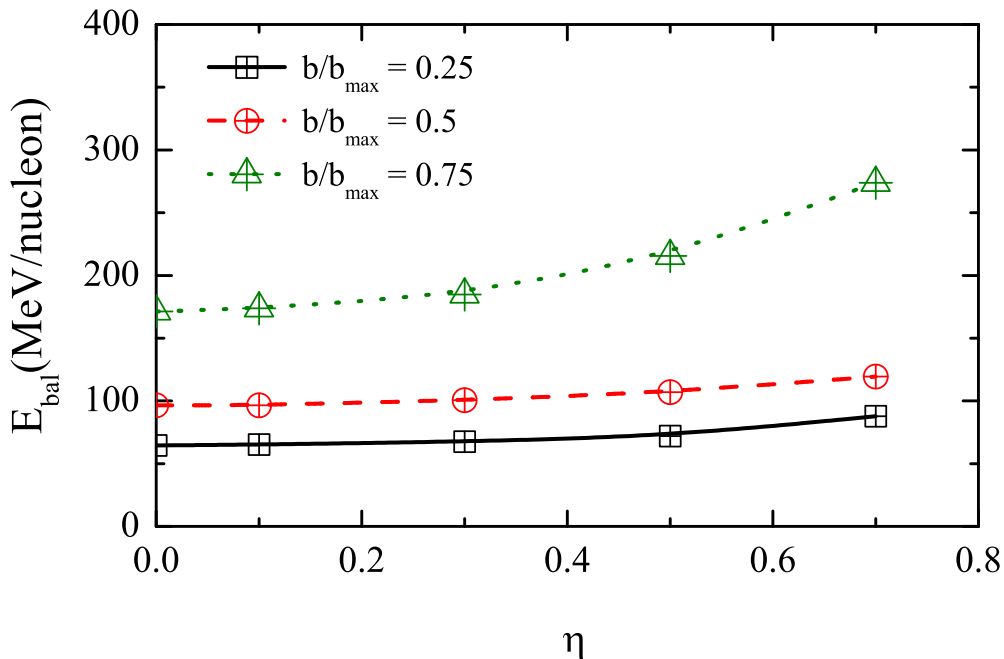**Figure 5.** (Color online) The E_{bal} as a function of η for system mass $A_{TOT} = 240$. The results for different impact parameters $b/b_{max} = 0.25$, 0.5, and 0.75 are represented, respectively, by the crossed squares, circles, and triangles. Lines are to guide the eye.

for other impact parameters also. The flow due to binary nn collisions, however, increases with increase in incident energy for all η, but as the impact parameter increases, the nn collision flow starts saturating. Obviously as explained earlier, the flow due to binary nn collisions decreases with increase in η.

In Fig. 5, we display E_{bal} as a function of η for $b/b_{max} = 0.25$, 0.5, and 0.75, keeping A_{TOT} fixed as 240. Various symbols are explained in the caption of the figure. From the figure, we see that E_{bal} increases with increase in η for all values of b/b_{max}. Also the η dependence of E_{bal} increases with increase in impact parameter.

In Fig. 6, we display the percentage change in balance energy $\Delta E_{bal}^{b/b_{max}}(\%)$, defined as $\Delta E_{bal}^{b/b_{max}}(\%) = ((E_{bal}^{b/b_{max}\neq0.25}\text{-}E_{bal}^{b/b_{max}=0.25})/E_{bal}^{b/b_{max}=0.25})\times100$ as a function of η. Lines represents the mean value of variation. It is clear from the figure that the effect of impact parameter variation is almost uniform throughout the asymmetry range for every fixed system mass. We also found that the mean variation decreases with increase in A_{TOT}. Clearly, the effect of impact parameter variation is independent of η.

In Fig. 7, we display the percentage difference $\Delta E_{bal}^{\eta}(\%)$ defined as $\Delta E_{bal}^{\eta}(\%) = ((E_{bal}^{\eta\neq0}$ - $E_{bal}^{\eta=0})/E_{bal}^{\eta=0})\times100$ as a function of reduced impact parameter (b/b_{max}). Lines are the linear fits $(\propto m\frac{b}{b_{max}})$. It is clear from the figure that the effect of the asymmetry variation increases with increase in the impact parameter for each mass range. This is due to the fact that with increase in impact parameter, the number of binary nn collisions decreases and the increase of mass asymmetry further adds the same effect.
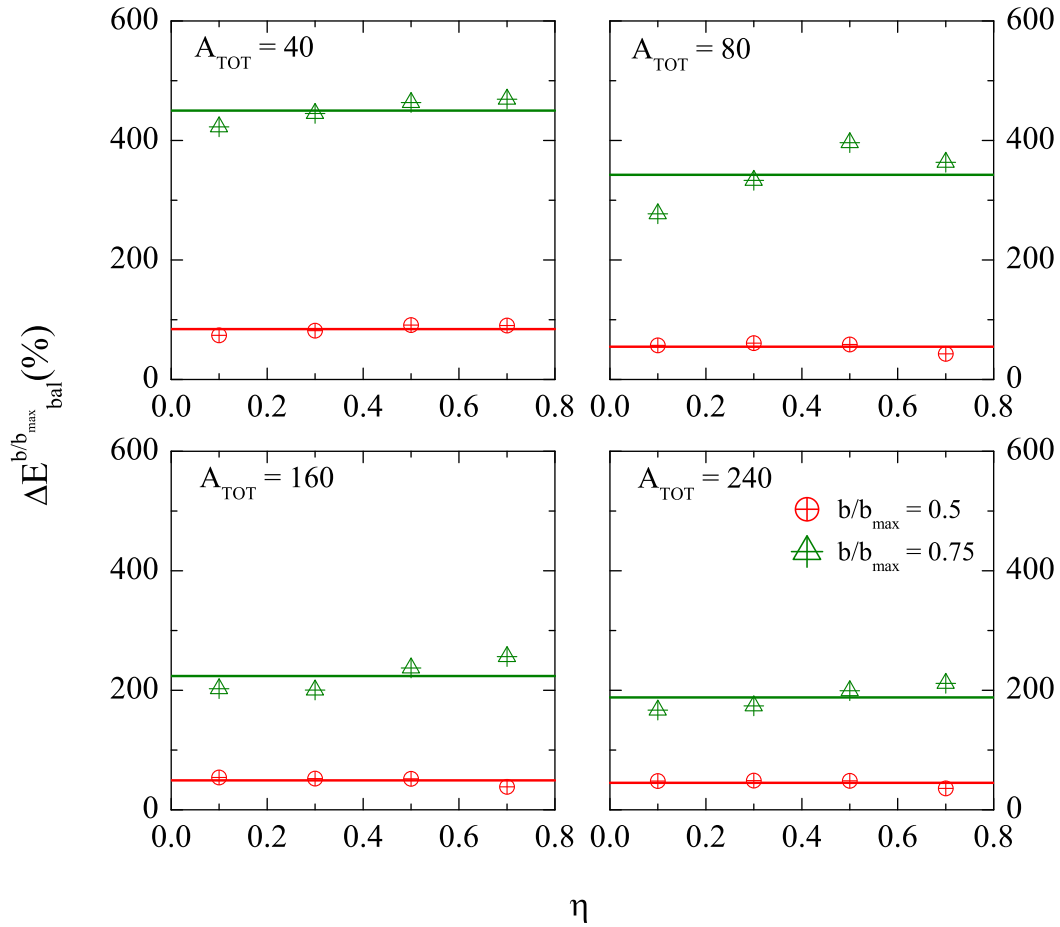
Figure 6. (Color online) The percentage difference $\Delta E_{bal}^{b/b_{max}}(\%)$ as a function of η for different system masses. The results of the percentage difference for different colliding geometries b/b_{max} = 0.5 and 0.75 are represented, respectively, by the crossed circles and triangles. Horizontal lines represent the mean value of $\Delta E_{bal}^{b/b_{max}}(\%)$ for each b/b_{max}.

4. Summary

We presented a detailed study on the role of impact parameter on the collective flow and its disappearance for different mass asymmetric reactions using the quantum molecular dynamics model. For the present study, the mass asymmetry of the reaction is varied from 0 to 0.7 by keeping the total mass of the system fixed. A significant role of impact parameter on the collective flow and its disappearance for the mass asymmetric reactions is seen. The impact parameter dependence is also found to vary with mass asymmetry of the reaction.

5. Acknowledgments

6. References

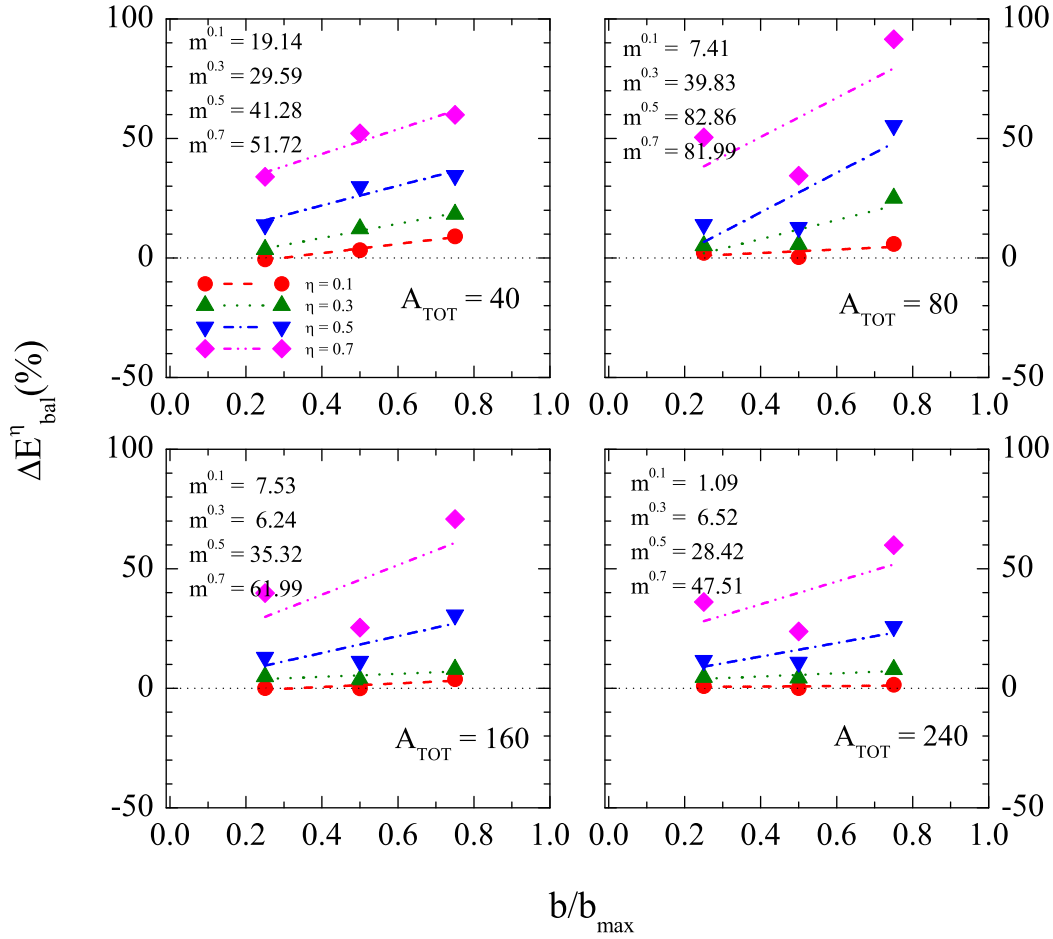[1] Krofcheck D *et al.* 1989 *Phys. Rev. Lett.* **63** 2028

Figure 7. (Color online) The percentage difference $\Delta E_{bal}^{\eta}(\%)$ as a function of b/b_{max} for different system masses. The results of the percentage difference for different asymmetries $\eta = 0.1$, 0.3, 0.5, and 0.7 are represented, respectively, by the solid circles, triangles, inverted triangles, and diamonds. Lines are the linear fits ($\propto m \frac{b}{b_{max}}$); m values without errors are displayed.

[2] Lukasik J *et al.* 2005 *Phys. Lett.* B **608** 223
[3] Mota la V de *et al.* 1992 *Phys. Rev.* C **677** 46
       Zhou H, Li Z and Zhuo Y 1994 *Phys. Rev.* C **50** R2664
       Cussol D *et al.* 2002 *Phys. Rev.* C **65** 044604
[4] Westfall G D *et al.* 1993 *Phys. Rev. Lett.* **71** 1986
[5] Pak R *et al.* 1996 *Phys. Rev.* C **53** R1469
[6] Magestro D J *et al.* 2000 *Phys. Rev.* C **61** 021602(R)
[7] Magestro D J *et al.* 2000 *Phys. Rev.* C **62** 041603(R)
[8] Sood A D and Puri R K 2004 *Phys. Lett.* B **594** 260
       Sood A D and Puri R K 2004 *Phys. Rev.* C **69** 054612
       Sood A D and Puri R K 2006 *Phys. Rev.* C **73** 067602
       Sood A D and Puri R K 2006 *Eur. Phys. J.* A **30** 571
[9] Sullivan J P *et al.* 1990 *Phys. Lett.* B **249** 8
[10] Buta A *et al.* 1995 *Nucl. Phys.* A **584** 397
[11] Goyal S and Puri R K 2011 *Nucl. Phys.* A **853** 164
[12] Hong B *et al.* 2000 *Phys. Rev.* C **66** 034901
[13] Chugh R and Puri R K 2010 *Phys. Rev.* C **82** 014603

[14] Chugh R and Puri R K 2010 *Int. J. Mod. Phys.* E **19** 2009

[15] Huang S W *et al.* 1993 *Phys. Lett.* B **298** 41
　　Huang S W *et al.* 1993 *Prog. Nucl. Part. Phys.* **30** 105
　　Lehmann E *et al.* 1993 *Prog. Nucl. Part. Phys.* **30** 219
　　Batko G *et al.* 1994 *J. Phys. G* **20** 461
　　Lehmann E *et al.* 1995 *Phys. Rev.* C **51** 2113
　　Fucks C 1996 *J. Phys. G* **22** 131
　　Puri R K *et al.* 1996 *Phys. Rev.* C **54** 28
　　Kumar S *et al.* 1998 *Phys. Rev.* C **58** 3494
　　Hartnack C *et al.* 1998 *Eur. Phys. J.* A **1** 151
　　Kumar S *et al.* 1998 *Phys. Rev.* C **57** 2744
　　Puri R K *et al.* 2000 *J. Comp. Phys.* **162** 245
　　Sood A D and Puri R K 2004 *Phys. Rev.* C **70** 034611
　　Dhawan J K *et al.* 2007 *Phys. Rev.* C **75** 057610
　　Kumar S *et al.* 2008 *Phys. Rev.* C **78** 064602
　　Sood A D *et al.* 2009 *Phys. Rev.* C **79** 064618
　　Vermani Y K *et al.* 2009 *Eur. Phys. Lett.* **85** 062001
　　Vermani Y K *et al.* 2009 *J. Phys. G* **36** 105103
　　Sood A D *et al.* 2010 *Phys. Rev.* C **82** 014603
　　Kumar S *et al.* 2010 *Phys. Rev.* C **81** 014611
　　Kumar S *et al.* 2010 *Phys. Rev.* C **81** 014601
　　Vermani Y K *et al.* 2010 *J. Phys. G* **37** 015105
　　Gautam S *et al.* 2010 *J. Phys. G* **37** 085102
　　Gautam S *et al.* 2011 *Phys. Rev.* C **83** 014603
　　Gautam S *et al.* 2011 *Phys. Rev.* C **83** 034606
　　Hauer W *et al.* 2011 *Phys. Lett.* B **697** 512
　　Goyal S and Puri R K 2011 *Phys. Rev.* C **83** 047601

[16] Aichelin J 1991 *Phys. Rep.* **202** 233

[17] Puri R K *et al.* 1991 *Phys. Rev.* C **43** 315
　　Puri R K *et al.* 1997 *Phys. Rev.* C **45** 1837
　　Puri R K *et al.* 1998 *Eur. Phys. J.* A **3** 277
　　Puri R K *et al.* 2000 *Eur. Phys. J.* A **8** 103
　　Puri R K *et al.* 2005 *Eur. Phys. J.* A **23** 429
　　Dutt I *et al.* 2010 *Phys. Rev.* C **81** 044615
　　Dutt I *et al.* 2010 *Phys. Rev.* C **81** 047601
　　Dutt I *et al.* 2010 *Phys. Rev.* C **81** 064609
　　Dutt I *et al.* 2010 *Phys. Rev.* C **81** 064608
　　Kumar S *et al.* 2010 *Chinese Phys. Lett.* **27** 062504

[18] Chugh R and Sood A D 2011 *arXiv:1010.1120v2*